# Efficacy of a resveratrol nanoformulation based on a commercially available liposomal platform

Carla Caddeo [a,*], Daniela Lucchesi [b], Xavier Fernàndez-Busquets [c,d], Donatella Valenti [a], Giuseppe Penno [b], Anna Maria Fadda [a], Laura Pucci [e,*]

[a] Dept. of Scienze della Vita e dell'Ambiente, Sezione di Scienze del Farmaco, University of Cagliari, Via Ospedale 72, 09124 Cagliari, Italy

[b] Dept. of Clinical and Experimental Medicine, Section of Diabetes and Metabolic Diseases, University of Pisa, via Piero Trivella, 56124 Pisa, Italy

[c] Nanomalaria Group, Institute for Bioengineering of Catalonia (IBEC), The Barcelona Institute of Science and Technology, Baldiri Reixac 10-12, Barcelona E08028, Spain

[d] Barcelona Institute for Global Health (ISGlobal), Hospital Clínic-Universitat de Barcelona, Rosselló 149-153, Barcelona E08036, Spain

[e] Institute of Agricultural Biology and Biotechnology, CNR Pisa, Via Moruzzi 1, 56124 Pisa, Italy

* Corresponding authors:

Carla Caddeo

Dept. of Scienze della Vita e dell'Ambiente, Sezione di Scienze del Farmaco, University of Cagliari, Via Ospedale 72, 09124 Cagliari, Italy

Tel.: +39 0706758462; fax: +39 0706758553; e-mail address: caddeoc@unica.it

Laura Pucci

Institute of Agricultural Biology and Biotechnology, CNR Pisa, Via Moruzzi 1, 56124 Pisa, Italy

Tel.: +39 0503153084; e-mail address: laura.pucci@ibba.cnr.it

**ABSTRACT**

Scalability is one of the important factors slowing down or even impeding the clinical translation of nanoparticle-based systems. The latter need to be manufactured at a high level of quality, with batch-to-batch reproducibility, and need to be stable after the manufacturing process, during long-term storage and upon clinical administration. In this study, a vesicular formulation intended for cutaneous applications was developed by the easy reconstitution of a commercially available liposomal platform. Resveratrol, a naturally occurring compound with potent antioxidant activity, and Tween80, a hydrophilic non-ionic surfactant, were included in the formulation. The physico-chemical properties of the vesicles were assessed using light scattering and cryogenic transmission electron microscopy. Nanosized (around 80 nm) spherical and elongated, unilamellar vesicles were produced, with remarkable storage stability. The incorporation of resveratrol in the vesicular system did not alter its strong antioxidant activity, as demonstrated by antioxidant colorimetric assays (DPPH and FRAP). Furthermore, the resveratrol liposomes were cytocompatible with fibroblasts and capable of protecting skin cells from oxidative stress by reducing both endogenous and chemically induced reactive oxygen species more effectively than free resveratrol. Therefore, the proposed formulation, based on the use of a commercially available liposomal platform, represents an easy-to-prepare, reproducible, up-scaled and efficient means of delivering resveratrol and potentiating its biological activity *in vitro*.

**Keywords:** resveratrol; commercial liposomes; skin delivery; skin cells; antioxidant.

## 1. Introduction

New strategies, accessible approaches and technologies are still needed to develop safe and successful therapies. Many untapped and potentially therapeutic molecules with reduced side effects can be found in traditional herbal medicines and foods (Liu, 2013; Pan et al., 2013; Veselkov et al., 2019). Natural compounds such as resveratrol have attracted significant interest in the pharmaceutical research due to their numerous health-promoting effects, coupled with their safety profiles and natural origins (Caddeo et al., 2015; Salehi et al., 2018). Unfortunately, the beneficial use of resveratrol's biological activities is hampered by its low aqueous solubility, chemical instability and rapid metabolism (Ahmadi and Ebrahimzadeh, 2020; Gligorijević et al., 2021). The incorporation of such compounds into liposomes is a well-known and effective approach to overcoming such limitations, with a consequent enhancement of the bioavailability of the payload (Daraee et al., 2016; Lee, 2020).

Liposomes are the most successful commercial nanosized drug delivery system. They were the first nanoparticle-based system to get regulatory approval for clinical use, and are still the most widely used platform for marketed pharmaceutical products, as well as the best-investigated platform in clinical trials and academic research (Sercombe et al., 2015; Zylberberg and Matosevic, 2016; Nisini et al., 2018; Jensen and Hodgson, 2020).

One of the important factors slowing down or even impeding the clinical translation of nanoparticle-based systems is the scalability of the formulations. Platforms that require complex and/or laborious production procedures generally have limited clinical translation potential, as they can be problematic to manufacture on a large scale (Hua et al., 2018). Besides the need for large, scalable quantities, formulations need to be manufactured at a high level of quality, with batch-to-batch reproducibility, and need to be stable after the manufacturing process, during long-term storage and upon clinical administration.

As already described, liposomes have been successfully developed on an industrial scale, without the need for multiple manufacturing steps or the use of organic solvents (Jaafar-Maalej et al., 2012; Kraft et al., 2014). Challenges arise when liposome systems become more complex, as the presence of multiple components inevitably poses manufacturing and production problems, increases costs, and makes quality assurance and quality control evaluation more difficult (Svenson, 2012; Tinkle et al., 2014). They may also lead to significant changes in the physico-chemical properties, pharmacokinetic profiles, and pharmacodynamic interactions (Hua et al., 2018). Hence, a balance between the complexity of the formulation design, the therapeutic efficacy and the clinical translation is needed.

In light of these considerations, in this study, we have developed a novel vesicular formulation using a commercially available liposomal platform, which is produced on a large scale and which meets quality, safety and reproducibility requirements. The vesicular formulation was optimised for the loading and delivery of resveratrol and characterised to assess its main physico-chemical and technological properties. Additionally, the biocompatibility and antioxidant activity of the resveratrol formulation were investigated in skin cells, with the purpose of assessing the enhanced efficacy of the vesicular delivery.

## 2. Materials and methods

### *2.1. Materials*

Pronanosome LIPO-N ready-to-use powder vesicles were kindly provided by Nanovex Biotechnologies SL (Llanera, Spain). Tween 80 was purchased from Galeno (Carmignano, Prato, Italy); resveratrol (RSV) and all other reagents, if not otherwise specified, were purchased from Sigma-Aldrich/Merck (Milan, Italy).

### *2.2. Vesicle preparation and characterisation*

Resveratrol (2 mg/ml) and Tween 80 (10 mg/ml) were weighed in a ready-to-use glass vial containing Pronanosome LIPO-N in its dried form (100 mg) and dispersed in water (2 ml; Table 1). To reconstitute the vesicles, the dispersion was hand-shaken, left to hydrate overnight and sonicated (5 sec on and 2 sec off, 20 cycles; 13 microns of probe amplitude) with a Soniprep 150 (MSE Crowley, London, UK).

For comparative purposes, empty vesicles were prepared following the above procedure, but without the addition of resveratrol (Table 1).

All the samples were prepared and kept in the dark for the duration of the experiments.

Vesicle formation and morphology were examined using cryogenic-transmission electron microscopy (cryo-TEM). For the analysis, a thin aqueous film was formed by placing 5 µl of the vesicular dispersion on a glow-discharged holey carbon grid and then blotting the grid against filter paper. The resulting thin sample film spanning the grid holes was vitrified by plunging the grid (kept at 100% humidity and room temperature) into ethane, maintained at its melting point with liquid nitrogen using a Vitrobot (FEI Company, Eindhoven, The Netherlands). The vitreous film was transferred to a Tecnai F20 TEM (FEI Company) using a Gatan cryo-transfer (Gatan, Pleasanton, CA, US), and the sample was observed in a low-dose mode. Images were acquired at 200 kV at a temperature of –170/–175 °C, using low-dose imaging conditions not exceeding 20 $e^{-}$ /$Å^2$, with a 4096 × 4096 pixel CCD Eagle camera (FEI Company).

The average diameter, polydispersity index (PI, a measure of the width of size distribution) and zeta potential of the vesicles were determined via dynamic and electrophoretic light scattering using a Zetasizer nano-ZS (Malvern Panalytical, Worcestershire, UK). Samples ($n > 6$) were diluted with water (1:100) and analysed at 25 °C.

The vesicle dispersions were purified from the non-incorporated resveratrol by dialysis. Each sample (1 ml) was loaded into Spectra/Por® tubing (12–14 kDa MW cut-off; Spectrum Laboratories Inc., DG Breda, The Netherlands), previously rinsed in water, and dialysed against water (2 l) for 2

144 h to allow the removal of the non-incorporated resveratrol. After disruption of unpurified and
145 purified vesicles with methanol, the entrapment efficiency (E), expressed as the percentage of the
146 amount of resveratrol detected in unpurified samples, was determined by high performance liquid
147 chromatography (Alliance 2690, Waters, Milan, Italy). Resveratrol content was assayed using a
148 XSelect C18 column (3.5 µm, 4.6×150 mm, Waters), with a mobile phase consisting of methanol,
149 acetonitrile, water and acetic acid (75:22.5:2.4:0.1, v/v) at a flow rate of 0.8 ml/min. $A_{306}$ was
150 measured for resveratrol quantification.
151 The stability of the formulations was evaluated by monitoring vesicle mean size, PI, zeta potential
152 and resveratrol content over three months at 4 ± 2 °C.
153
154 *2.3. Antioxidant activity: DPPH and FRAP assays*The antioxidant activity of the resveratrol
155 formulations was assessed by evaluating their ability to scavenge 2,2-diphenyl-1-picrylhydrazyl
156 (DPPH), a stable nitrogen-centered free radical. DPPH was dissolved in methanol to yield a 25 µM
157 concentration, and the solution (2 ml) was mixed with 20 µl of each sample (i.e., empty vesicles,
158 resveratrol vesicles, resveratrol methanolic solution), and stored at room temperature for 30 min, in
159 the dark. Thereafter, the absorbance was measured at 517 nm against blank. The extent of
160 discoloration of the violet colour of DPPH methanolic solution, quantified as a decrease in
161 absorbance, depends on the intrinsic antioxidant activity/radical scavenging activity and
162 concentration of a sample. Antioxidant compounds can neutralize the DPPH radical by either direct
163 reduction via electron donation or by radical quenching via hydrogen atom donation.The DPPH
164 radical scavenging activity of each sample was expressed as (i) percent antioxidant activity (AA)
165 calculated according to the following formula, where A is the absorbance:
166 $$AA = \left( \frac{A_{DPPH} - A_{sample}}{A_{DPPH}} \right) x100$$

and (ii) as Trolox equivalent antioxidant capacity (TEAC). The TEAC values were calculated based on a calibration curve plotted using Trolox (reference standard) at different concentrations (0.1–1 mg/ml). Results were expressed as mg Trolox equivalents/ml solution. TEAC reflects the ability of antioxidant samples to scavenge DPPH radical as compared with that of Trolox: the higher the TEAC values, the higher the radical scavenging activity of the samples.

The antioxidant activity was also assessed by the FRAP (ferric reducing antioxidant power) assay, which evaluates antioxidants as reductants of $Fe^{3+}$ to $Fe^{2+}$: $Fe^{3+}$ is chelated by 2,4,6-tris(pyridin-2-yl)-1,3,5-triazine (TPTZ) to form a $Fe^{2+}$–TPTZ blue-coloured complex that increases the absorption at 593 nm (Tuberoso et al., 2013). A ferric complex solution was freshly prepared with TPTZ and $Fe^{3+}$ (0.3123 g TPTZ, 0.5406 g $FeCl_3$ $6H_2O$ in 100 ml acetate buffer pH 3.6). 20 µl of each sample (i.e., empty vesicles, resveratrol vesicles, resveratrol methanolic solution) was dissolved in 2 ml of the ferric complex solution and incubated for 4 min in the dark; absorbance at 593 nm was measured with a spectrophotometer. Quantitative analysis was performed according to the external standard method ($FeSO_4$, mg/ml), correlating the absorbance of the samples with the $FeSO_4$ concentration, and results were expressed as ferrous equivalents (mg $Fe^{2+}$ equivalents (FE)/ml solution).

*2.4. Fibroblast cell culture*

3T3-L1 cells (ATCC®CL-173TM) were grown in Dulbecco's modified Eagle's medium (DMEM) supplemented with 10% fetal bovine serum (FBS), 100 units/ml penicillin, and 100 µg/ml streptomycin, and maintained at 37 °C in a humidified 5% $CO_2$ incubator. The cells were seeded into 96-well plates and tested under the following experimental conditions:

1. cells unexposed (control) or exposed to 250 µM 2,2′ -azobis(2-methylpropionamidine) dihydrochloride (AAPH, a peroxyl radical generator used as a positive control) for 4 h;

2. cells exposed to resveratrol liposomes or resveratrol ethanolic solution, previously diluted to reach the required doses of resveratrol (0.01, 0.1, 1.0 and 10 μg/well), for 5 h;

3. cells exposed to resveratrol liposomes or resveratrol ethanolic solution, previously diluted to reach the required doses of resveratrol (0.01, 0.1, 1.0 and 10 μg/well), for 1 h and co-incubated with 250 μM AAPH for a further 4 h. For comparative purposes, empty liposomes were tested at the same dilutions as the resveratrol liposomes or ethanolic solution.

*2.5. Assessment of viability*

The MTT assay was performed to evaluate the viability of cultured 3T3-L1 cells upon different treatment conditions (see Section 2.4). MTT (3-(4,5-dimethylthiazol-2-yl)-2,5-diphenyltetrazolium bromide) reagent (Sigma, St. Louis, MO, USA) measures mitochondrial activity in live cells. Briefly, fibroblasts ($5\times10^4$ cells/well) were incubated with MTT (0.5 mg/ml) for 3 h at 37 °C in 5% $CO_2$. After incubation, the medium was removed, and the cells solubilised in 10% DMSO/90% isopropanol. Then, the amount of the dye released from the cells was quantified by measuring the optical density at 540 nm (reference wavelength: 620 nm) by using a multiplate reader (Multiskan EX, Thermo Fisher Scientific, Waltham, MA, US). The experiment was repeated at least three times independently, each time in triplicate.

Results are expressed as percentage vs. control cells viability.

*2.6. Assessment of cellular reactive oxygen species (ROS)*

After incubation of 3T3-L1 cells with the samples or the samples and 250 μM AAPH (see Section 2.4), endogenous or chemically-induced cellular ROS were detected using 5-(and-6)-chloromethyl-2',7'-dichlorodihydrofluorescein diacetate, acetyl ester (CM-$H_2$DCF-DA; Invitrogen, Life Technologies Ltd, Thermo Fisher Scientific, Waltham, MA, US) fluorescent probe.

Briefly, 3T3-L1 cells, seeded at a density of $5\times10^4$ cells/well into a 96-well blackened fluorescence plate, were incubated with CM-$H_2$DCF-DA (5 μM/well) for 60 min at 37 °C in the dark. Afterwards, the cells were rinsed with 1× PBS to remove CM-$H_2$DCF-DA solution and treated according to the experimental conditions reported in Section 2.4.

ROS production was detected by measuring fluorescence intensity at 485 nm excitation and 520 nm emission using a FLUOstar® Omega multi-mode microplate reader. The fluorescence plate reader measures the light signal emitted by a sample in Relative Fluorescent Units (RFU). The experiment was repeated at least three times independently, each time in triplicate. Results are expressed as percentage vs. control cells ROS production.

3T3-L1 cells (CTR), untreated or incubated with 250 μM AAPH, or co-incubated with 250 μM AAPH and empty liposomes, resveratrol solution, resveratrol liposomes for 5 h were examined under a Primo Vert inverted microscope (Carl Zeiss Microscopy GmbH, Jena, Germany) to assess cell morphology.

### *2.7. Statistical analysis of data*

Results are expressed as the mean ± standard deviation (SD). Statistical analysis of data was performed using StatView software package (SAS Institute Inc., Cary, NC, US) by one-way analysis of variance (ANOVA). Fisher's post-hoc test was used for single comparisons. *P* values <0.05 were considered as statistically significant.

## 3. Results and discussion

### *3.1. Vesicle design and characterization*

The present study was aimed at developing a vesicular formulation for the delivery of resveratrol to the skin. A commercial liposomal platform, Pronanosome LIPO-N, was used for the preparation of small, reproducible, and stable liposomes. Given their versatility and ease of use, Pronanosome

LIPO-N can be loaded with any bioactive compound. In this work, Pronanosome LIPO-N were loaded with resveratrol, a natural polyphenol with countless biological activities.

In order to discriminate between the effect of the carrier and the polyphenol, resveratrol liposomes were prepared, characterised and tested *in vitro* in comparison with empty liposomes.

Light scattering results, summarised in Table 2, showed that empty liposomes were small in size (~80 nm). These liposomes were also characterized by high homogeneity (PI 0.22), and negative zeta potential (–25 mV), due to the charge carried by the proprietary Pronanosome LIPO-N phospholipid mixture. The loading of resveratrol did not alter these values ($p$>0.05), with the exception of the PI value, which was lower (0.19; $p$<0.05). This finding was indicative of an even higher homogeneity of the vesicle formulation.

The entrapment efficiency of the liposomes was high (83%; Table 2), and the amount of the loaded resveratrol did not diminish during a three-month- storage period ($p$>0.05). This aligns with previous results showing that resveratrol is efficiently loaded in phospholipid vesicles (Caddeo et al., 2018; Caddeo et al., 2021).

Cryo-TEM observation of resveratrol liposomes confirmed the formation of small unilamellar vesicles, either spherical or elongated (Fig. 1); no evidence of free resveratrol crystals was seen.

As known, the stability of a nanoparticle-based formulation is critical to ensure its use is both safe and effective. The stability of the resveratrol formulation was evaluated by monitoring the mean diameter, PI and zeta potential of the vesicles over three months of storage. As the results show in Fig. 2, no significant variations were found among the three examined parameters ($p$>0.05).

### *3.3. Antioxidant assays*

Antioxidant activity of the resveratrol formulation was assessed by evaluating its ability to scavenge radical species (DPPH assay) and reduce ferric ions (FRAP assay).

The DPPH assay exploits the reduction of the DPPH free radical in the presence of antioxidant molecules such as resveratrol. The results of the assay are summarised in Table 3. The DPPH radical was almost completely scavenged (87%). Given the strong antioxidant power of resveratrol, this was expected. It is worth noting that the antioxidant activity of resveratrol in liposomes was essentially the same (84%; $p>0.05$), corresponding to ~320 μg/ml of Trolox equivalents. This demonstrated that incorporation in the vesicle system did not alter the inner properties of the polyphenol.

The FRAP assay exploits the reduction of $Fe^{3+}$ by antioxidant molecules. The results obtained from the assay showed the same trend; the resveratrol liposomes displayed a reduction potential as strong as that of free resveratrol, which was around 8 mg/ml of ferrous equivalents (Table 3). These findings confirm that the antioxidant activity of resveratrol was retained in the vesicle formulation.

*3.4. Cell viability*

To assess the effect of the vesicular formulation on 3T3-L1 fibroblasts, we evaluated cell viability in both the presence and absence of AAPH-induced oxidative stress. 3T3-L1 fibroblasts were incubated with 0, 100, 250, 500 and 1000 μM AAPH for 4 h, and the concentration that triggered ROS production without significantly reducing cell viability was determined. Given the results reported in Fig. 3, it was shown that 100 μM AAPH did not reduce cell viability. However, 500 and 1000 μM AAPH concentrations were too strong, and they resulted in a 30% mortality rate. A proper concentration of 250 μM AAPH was selected for the assessment of cell viability and intracellular ROS production under stress conditions.

The absence of cytotoxic effects of the formulations was evaluated in 3T3-L1 fibroblasts in terms of viability. This followed 5 h of exposure to increasing doses of resveratrol ranging from 0.01 to 10 μg (Fig. 4). Analysis of variance showed a significant difference between groups after 5 h exposure ($p<0.0001$). After this time, cytotoxicity was significantly induced by the higher testing dose of

289 resveratrol solution (10 μg; $p < 0.0001$ vs. control); this resulted in a mortality rate of 82.1%. Such
290 decrease in viability was prevented by liposomes; the mortality rate of cells exposed to resveratrol
291 liposomes (10 μg; $p < 0.0001$ vs. control) was 55%. The protection offered by the nanocarrier was
292 confirmed by the low mortality (27.4%; $p = 0.0144$ vs. control) of cells exposed to empty
293 liposomes, which were tested at the same dilution used to reach 10 μg resveratrol.
294 In the presence of 250 μM AAPH, the same behaviour was observed (Fig. 4). Cell viability was
295 significantly reduced only in the case of exposure to the higher dose of resveratrol. This confirmed
296 the mortality values found under non-stress conditions: 82.3% with resveratrol solution ($p<0.0001$
297 vs. 250 μM AAPH), 54.4% with resveratrol liposomes ($p<0.0001$ vs. 250 μM AAPH), and 34.2%
298 with empty liposomes ($p=0.0024$ vs. 250 μM AAPH).
299 Therefore, the effects of spontaneous and induced oxidative stress were superimposable. The results
300 point to the ability of liposomes to protect the cells from the inner toxicity of high doses of
301 resveratrol that lead to cell death. This aligns with previous studies showing that resveratrol can act
302 as either an antioxidant or a pro-oxidant agent. Aside from the treatment conditions, the specific
303 microenvironment, the type of cells, and their basal redox state, this depends on the concentration
304 used (Alarcón de la Lastra and Villegas, 2007; Khan et al., 2013). Dose-dependent effects have
305 been described. At low concentrations, resveratrol acts as an antioxidant that can protect from DNA
306 damage and oxidative stress. At high concentrations, it acts as a pro-oxidant that promotes DNA
307 damage and increases oxidative stress (Calabrese et al., 2010; Shaito et al., 2020).
308
309 *3.5. Intracellular ROS production*
310 The antioxidant activity of the resveratrol formulation was analysed in AAPH-stressed 3T3-L1 skin
311 cells as a reducer of ROS levels. This was performed by using DCFH-DA, a cell-permeable dye
312 sensitive to the cellular redox state.

A total of 5 h of exposure was performed with resveratrol solution, empty liposomes, and resveratrol liposomes in the absence of AAPH in cell culture. Aside from when cells were incubated with the higher dose of empty liposomes, no increase in spontaneous ROS production was detected (Fig. 5).

The incubation of cells with 250 µM AAPH significantly triggered ROS production (50% increase; $p < 0.0001$ vs. control). The treatment with empty liposomes at higher doses caused a further increase in the cellular ROS levels (Fig. 5). On the other hand, a statistically significant dose-dependent decrease in ROS levels was found upon exposure to resveratrol solution. Similarly, a significant decrease in ROS was observed upon treatment with resveratrol liposomes, which restored the basal levels at the higher dose (10 µg; $p < 0.0001$ vs. 250 µM AAPH).

The low levels of ROS detected in cells treated with 10 µg resveratrol solution were seemingly comparable to those detected in untreated control cells (Fig. 5). However, this was not due to the antioxidant activity of resveratrol; the low levels were attributed to the reduced number of live cells. Indeed, as displayed by the viability data reported in Fig. 4, a 10 µg resveratrol solution caused an 82% cell mortality rate. This result was confirmed by the images obtained with an inverted microscope (Fig. 6). It was shown that the application of the higher dose of resveratrol solution in AAPH-exposed cells was clearly associated with a significant cell death. This, in turn, leads to lower ROS levels. However, in terms of morphology and number, it was apparent that cells treated with the same dose of resveratrol liposomes (i.e., 10 µg) displayed features similar to untreated cells (Fig. 6).

## 4. Conclusions

The results of the present work demonstrated that the resveratrol formulation developed by using a commercially available liposomal platform ensured the requirements of quality, reproducibility, and

efficiency. The liposomes were small in size, highly stable, and effective in preserving the antioxidant activity of resveratrol and reducing its cytotoxicity at high doses.

Therefore, these findings respond to the need to develop scalable formulations characterized by high quality, safety, and effectiveness. Further research, such as targeted *in vivo* tests, are needed to validate the *in vitro* potential of the resveratrol formulation for clinical translation.

**Acknowledgments**

The Authors would like to thank Nanovex Biotechnologies SL (Parque Tecnológico de Asturias, CEEI, 33428 Llanera, Asturias, Spain) for kindly providing Pronanosome LIPO-N.

This research was partially supported by the following grants: RASSR14371 under FSC 2014-2020 program - Patto per lo Sviluppo della Regione Sardegna; RTI2018-094579-B-I00 (Spanish Ministry of Science, Innovation and Universities, Spain), which included FEDER funds; and 2017-SGR-908 (Generalitat de Catalunya, Spain).

ISGlobal and IBEC are members of the CERCA Programme, *Generalitat de Catalunya*. We acknowledge support from the Spanish Ministry of Science, Innovation and Universities through the *"Centro de Excelencia Severo Ochoa 2019-2023"* Program (CEX2018-000806-S). This research is part of ISGlobal's Program on the Molecular Mechanisms of Malaria which is partially supported by the *Fundación Ramón Areces*.

## References


Liu, R.H., 2013. Dietary bioactive compounds and their health implications. J. Food Science 78, S1.

Pan, S.-Y., Zhou, S.-F., Gao, S.-H., Yu, Z.-L., Zhang, S.-F., Tang, M.-K., Sun, J.-N., Ma, D.-L., Han, Y.-F., Fong, W.-F., Ko, K.-M., 2013. New perspectives on how to discover drugs from herbal medicines: CAM's outstanding contribution to modern therapeutics. Evid Based Complement. Alternat. Med. 627375.

Veselkov, K., Gonzalez, G., Aljifri, S., Galea, D., Mirnezami, R., Youssef, J., Bronstein, M., Laponogov, I., 2019. HyperFoods: machine intelligent mapping of cancer-beating molecules in foods. Scientific Reports 9, 9237.

Caddeo, C., Manconi, M., Cardia, M.C., Díez-Sales, O., Fadda, A.M., Sinico, C., 2015. Investigating the interactions of resveratrol with phospholipid vesicle bilayer and the skin: NMR studies and confocal imaging. Int. J. Pharm. 484, 138-145.

Salehi, B., Prakash Mishra, A., Nigam, M., Sener, B., Kilic, M., Sharifi-Rad, M., Valere Tsouh Fokou, P., Martins, N., Sharifi-Rad, J., 2018. Resveratrol: a double-edged sword in health benefits. Biomedicines 6(3), 91.

Ahmadi, R., Ebrahimzadeh, M.A., 2020. Resveratrol - A comprehensive review of recent advances in anticancer drug design and development. Eur. J. Med. Chem. 200, 112356.

Gligorijević, N., Stanić-Vučinić, D., Radomirović, M., Stojadinović, M., Khulal, U., Nedić, O., Ćirković Veličković, T., 2021. Role of resveratrol in prevention and control of cardiovascular disorders and cardiovascular complications related to COVID-19 disease: mode of action and approaches explored to increase its bioavailability. Molecules 26, 2834.

Daraee, H., Etemadi, A., Kouhi, M., Alimirzalu, S., Akbarzadeh, A., 2016. Application of liposomes in medicine and drug delivery. Artif. Cells Nanomed. Biotechnol 44, 381–391.

Lee, M.-K., 2020. Liposomes for enhanced bioavailability of water-insoluble drugs: in vivo evidence and recent approaches. Pharmaceutics 12(3), 264.

381 Sercombe, L., Veerati, T., Moheimani, F., Wu, S.Y., Sood, A.K., Hua, S., 2015. Advances and
382 challenges of liposome assisted drug delivery. Front. Pharmacol. 6, 286.
383 Zylberberg, C., Matosevic, S., 2016. Pharmaceutical liposomal drug delivery: a review of new
384 delivery systems and a look at the regulatory landscape. Drug Deliv. 23(9), 3319–3329.
385 Nisini, R., Poerio, N., Mariotti, S., De Santis, F., Fraziano, M., 2018. The multirole of liposomes in
386 therapy and prevention of infectious diseases. Front. Immunol., 9, 155.
387 Jensen, G.M., Hodgson, D.F., 2020. Opportunities and challenges in commercial pharmaceutical
388 liposome applications. Adv. Drug Deliv. Rev. 154–155, 2-12.
389 Hua, S., de Matos, M.B.C., Metselaar, J.M., Storm, G., 2018. Current trends and challenges in the
390 clinical translation of nanoparticulate nanomedicines: pathways for translational development and
391 commercialization. Front. Pharmacol. 9, 790.
392 Jaafar-Maalej, C., Elaissari, A., Fessi, H., 2012. Lipid-based carriers: manufacturing and
393 applications for pulmonary route. Expert Opin. Drug Deliv. 9, 1111–1127.
394 Kraft, J.C., Freeling, J.P., Wang, Z., Ho, R.J., 2014. Emerging research and clinical development
395 trends of liposome and lipid nanoparticle drug delivery systems. J. Pharm. Sci. 103, 29–52.
396 Svenson, S., 2012. Clinical translation of nanomedicines. Curr. Opin. Solid. State Mater. Sci. 16,
397 287–294.
398 Tinkle, S., McNeil, S.E., Muhlebach, S., Bawa, R., Borchard, G., Barenholz, Y.C., Tamarkin, L.,
399 Desai, N., 2014. Nanomedicines: addressing the scientific and regulatory gap. Ann. N. Y. Acad.
400 Sci. 1313, 35–56.
401 Tuberoso, C.I.G., Boban, M., Bifulco, E., Budimir, D., Pirisi, F.M., 2013. Antioxidant capacity and
402 vasodilatory properties of Mediterranean food: The case of Cannonau wine, myrtle berries liqueur
403 and strawberry-tree honey. Food Chem. 140, 686-691.

Caddeo, C., Pucci, L., Gabriele, M., Carbone, C., Fernàndez-Busquets, X., Valenti, D., Pons, R., Vassallo, A., Fadda, A.M., Manconi, M., 2018. Stability, biocompatibility and antioxidant activity of PEG-modified liposomes containing resveratrol. Int. J. Pharm. 538, 40–47.

Caddeo, C., Gabriele, M., Nacher, A., Fernandez-Busquets, X., Valenti, D., Fadda, A.M., Pucci, L., Manconi, M., 2021. Resveratrol and artemisinin eudragit-coated liposomes: A strategy to tackle intestinal tumors. Int. J. Pharm 592, 120083.

Alarcón de la Lastra, C., Villegas, I., 2007. Resveratrol as an antioxidant and pro-oxidant agent: mechanisms and clinical implications. Biochem. Soc. Trans. 35, part 5.

Khan, A., Chen, H., Wan, X., Tania, M., Xu, A., Chen, F., Zhang, D., 2013. Regulatory effects of resveratrol on antioxidant enzymes: a mechanism of growth inhibition and apoptosis induction in cancer cells. Mol. Cells 35, 219-225.

Calabrese, E.J., Mattson, M.P., Calabrese, V., 2010. Resveratrol commonly displays hormesis: occurrence and biomedical significance. Hum. Exp. Toxicol. 29, 980–1015.

Shaito, A., Posadino, A.M., Younes, N., Hasan, H., Halabi, S., Alhababi, D., Al-Mohannadi, A., Abdel-Rahman, W.M., Eid, A.H., Nasrallah, G.K., Pintus, G., 2020. Potential adverse effects of resveratrol: a literature review. Int. J. Mol. Sci. 21, 2084.

**Figure captions**

**Figure 1.** Cryo-TEM images of resveratrol liposomes.

**Figure 2.** Long-term stability of resveratrol liposomes assessed by monitoring mean diameter (MD), polydispersity index (PI) and zeta potential (ZP) for 90 days.

**Figure 3.** Effect of AAPH exposure on 3T3-L1 cells viability. Data are expressed as means ± SD; n=3. ** $p \leq 0.01$ vs. control (i.e., cells + 0 µM AAPH).

**Figure 4.** Cell viability in the absence or presence of oxidative stress induced by AAPH and upon exposure to empty liposomes, resveratrol solution, and resveratrol liposomes for 5 h. Data are expressed as means ± SD; n=³3. * $p<0.05$ vs. control; **** $p<0.0001$ vs. control; ### $p<0.005$ vs. 250 µM AAPH; #### <0.0001 vs. 250 µM AAPH.

**Figure 5.** Effects of 5 h exposure to empty liposomes, resveratrol solution, and resveratrol liposomes on ROS production in 3T3-L1 cells, in the absence or presence of AAPH induced-oxidative stress. Data are expressed as means of RFU (Relative Fluorescent Units) ± SD; n=³3. *$p<0.05$ vs. control; § $p<0.0001$ vs. control; # $p<0.05$ vs. 250 µM AAPH; ## $p \leq 0.01$ vs. 250 µM AAPH; ### $p<0.005$ vs. 250 µM AAPH; #### $p \leq 0.0001$ vs. 250 µM AAPH; ¤¤¤ $p \leq 0.0001$ vs. empty liposomes 10 µg + 250 µM AAPH; δδδ $p \leq 0.0001$ vs. empty liposomes 1 µg + 250 µM AAPH; ζζ $p=0.0005$ vs. empty liposomes 0.1 µg + 250 µM AAPH.

**Figure 6.** Representative microscope images of untreated 3T3-L1 cells (CTR), incubated with 250 µM AAPH, or incubated with 250 µM AAPH and exposed for 5 h to 10 µg empty liposomes, resveratrol solution, or resveratrol liposomes.

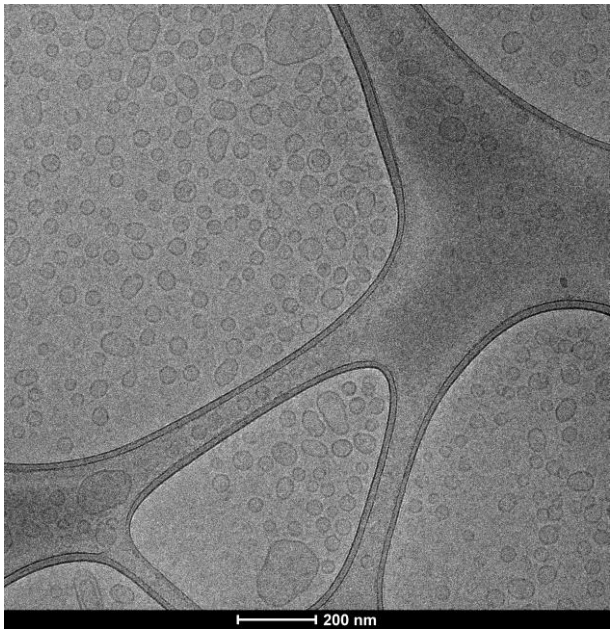


444

445

446

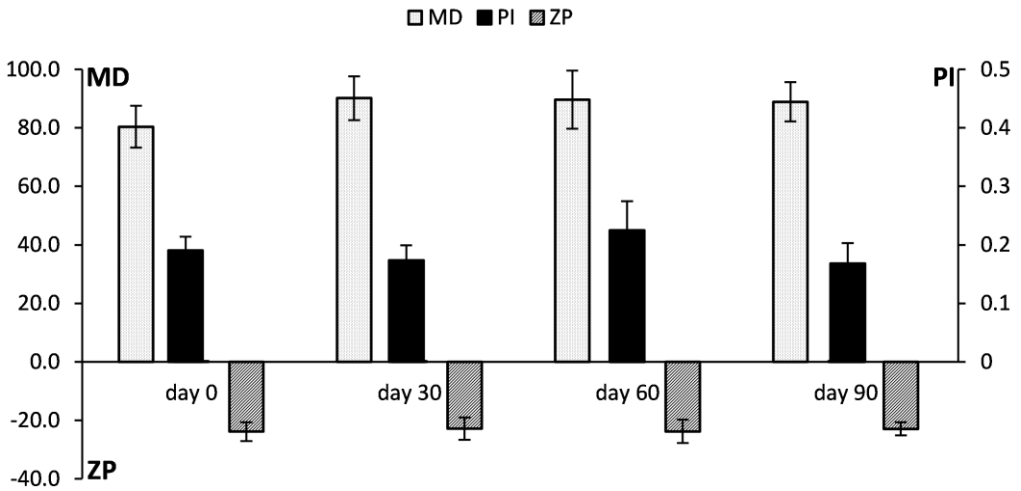


447

448

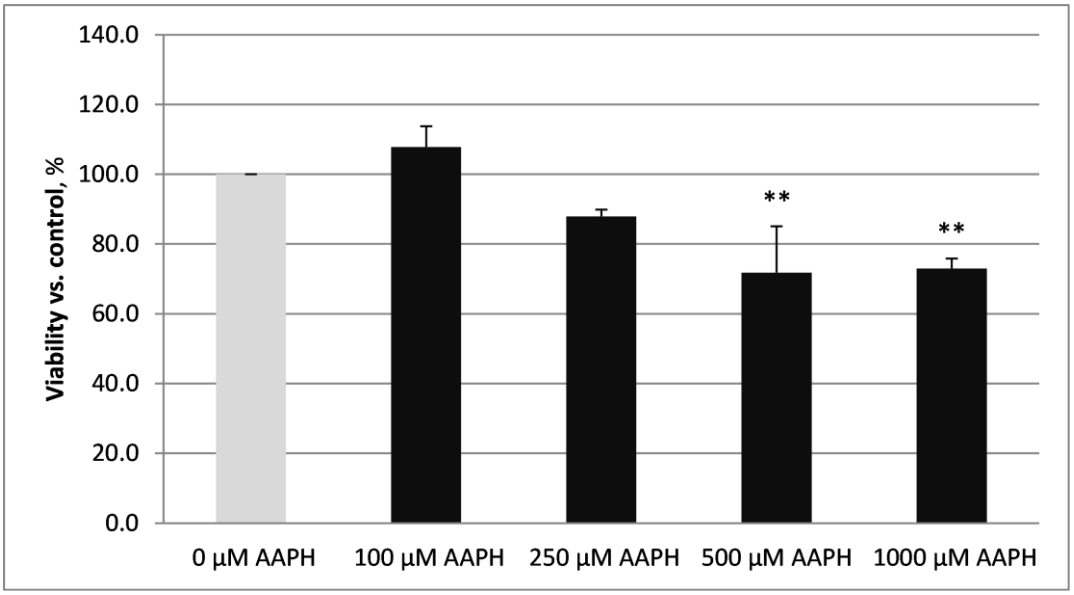


449

450

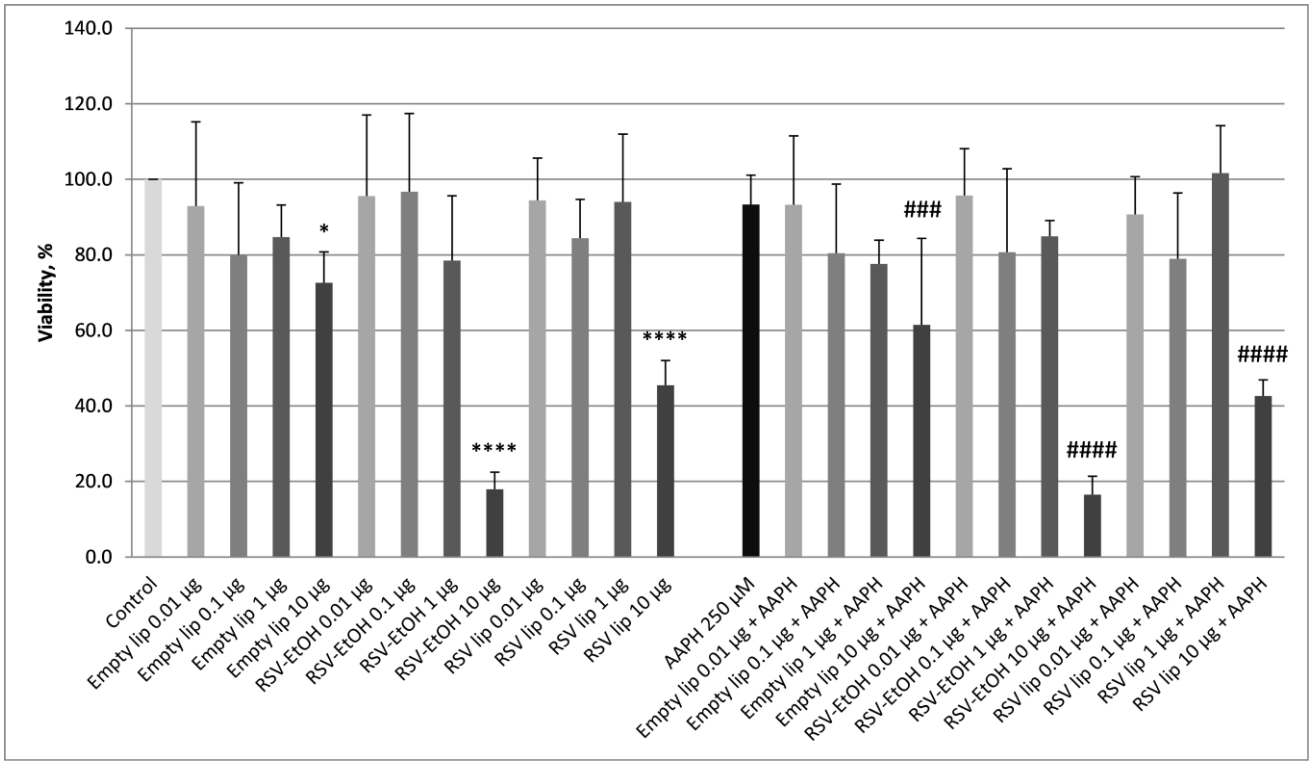


451

452

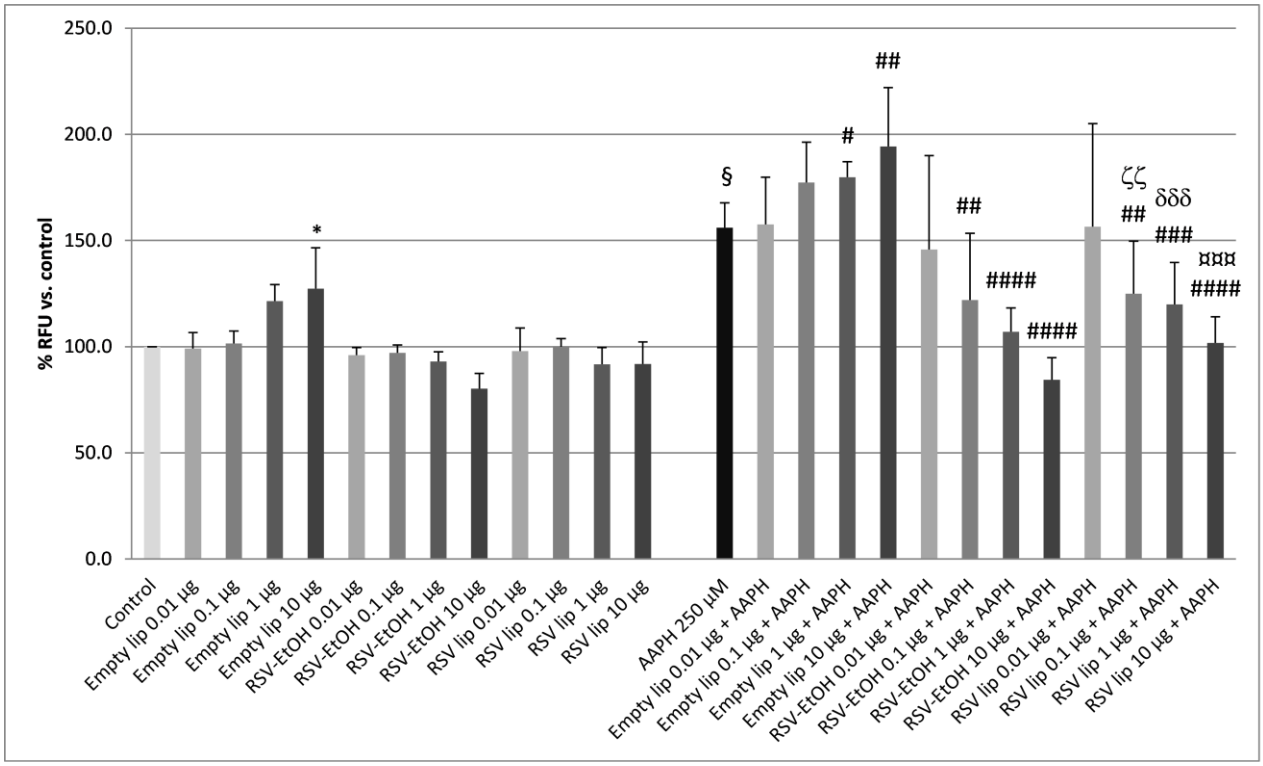


453

454

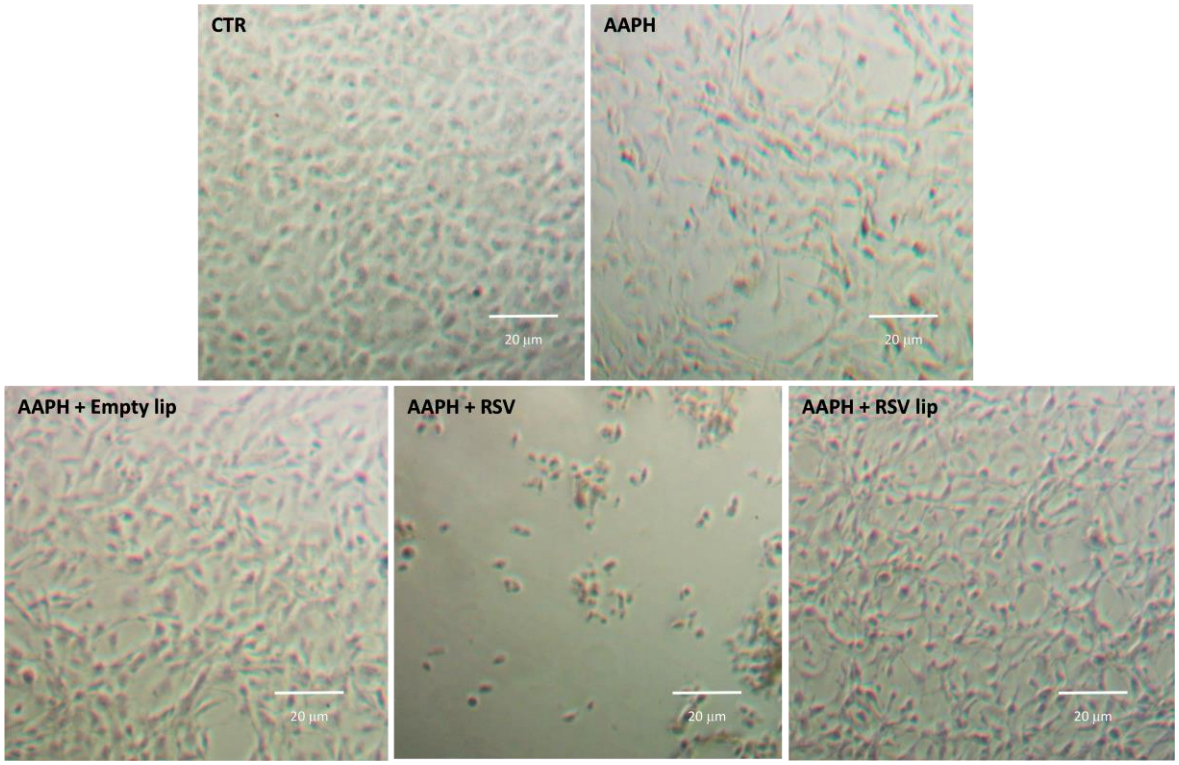


455

456

457

458 **Table 1.** Composition of the liposomal formulations.

| Formulation | LIPO-N | RSV | Tween80 | $H_2O$ |
|---|---|---|---|---|
| **Empty liposomes** | 100 mg | | 20 mg | 2 ml |
| **RSV liposomes** | 100 mg | 4 mg | 20 mg | 2 ml |

459

460

461 **Table 2.** Characteristics of empty and resveratrol (RSV) liposomes: mean diameter (MD),
462 polydispersity index (PI), zeta potential (ZP), and entrapment efficiency (E). Each value represents
463 the mean ± SD ($n \geq 6$). * values statistically different ($p<0.05$) from empty liposomes.

| Formulation | MD nm ± SD | PI | PZ mV ± SD | E % ± SD |
|---|---|---|---|---|
| **Empty liposomes** | 82 ± 4.4 | 0.22 ± 0.02 | –25 ± 3.2 | -- |
| **RSV liposomes** | 80 ± 7.2 | *0.19 ± 0.02 | –24 ± 3.2 | 83 ± 4.3 |

464

465

466 **Table 3.** *In vitro* antioxidant activity of resveratrol in the vesicle formulations in comparison with a
467 methanolic solution. DPPH results are expressed as AA (%) and as TEAC (μg/ml) concentration.
468 FRAP results are expressed as FE (μg/ml) concentration. Results are reported as the mean value ±
469 SD of 3 separate experiments, each performed in triplicate.

| Formulation | DPPH | | FRAP |
|---|---|---|---|
| | AA (%) | TEAC (μg of Trolox equivalents/ml) | FE (μg of $Fe^{2+}$ equivalents/ml) |
| **RSV in MeOH** | 87 ± 2.5 | 325 ± 3.3 | 8.8 ± 1.0 |
| **Empty liposomes** | 8 ± 1.6 | 165 ± 23 | 0.2 ± 0.002 |
| **RSV liposomes** | 84 ± 1.4 | 321 ± 7.0 | 8.1 ± 0.7 |

470